

## Lifetimes of negative parity states in $^{11}\text{C}$

A. Anttila, J. Keinonen, and R. Hentelä

*Department of Physics, University of Helsinki, 00170 Helsinki 17, Finland*

(Received 29 November 1978)

The lifetime limits  $\tau_m < 34$ ,  $< 12$ ,  $< 11$ ,  $< 8$ , and  $< 23$  fs for the negative parity states in  $^{11}\text{C}$ , at 2000, 4319, 4804, 6478, and 8425 keV, respectively, were determined with the Doppler shift attenuation method through the  $^{10}\text{B}(p,\gamma)^{11}\text{C}$  reaction. The analog of the  $^{11}\text{C}$  6478 keV state lies at 6743 keV in  $^{11}\text{B}$  and was measured to have a lifetime  $\tau_m = 15 \pm 6$  fs using the  $^7\text{Li}(\alpha,\gamma)^{11}\text{B}$  reaction. Experimentally obtained correction factors for the nuclear and electronic stopping powers were used in the Doppler shift attenuation analysis. In the calculations the Monte-Carlo method was employed. A new  $\gamma$ -ray decay scheme obtained for the  $^{10}\text{B}(p,\gamma)^{11}\text{C}$  reaction at  $E_p = 1110$  keV together with the angular distribution data illustrate that the properties of the resonant state reported to exist at  $E_x = 9.73$  MeV in  $^{11}\text{C}$  are strongly influenced by background processes and that the resonance structure is ambiguous. In the light of the new lifetime values, the transition strengths are discussed in terms of shell model calculations.

NUCLEAR REACTIONS  $^{10}\text{B}(p,\gamma)$ ,  $E = 1.11$  MeV;  $^7\text{Li}(\alpha,\gamma)$ ,  $E = 0.96$  MeV; measured  $E_\gamma$ ,  $I_\gamma(\theta)$ , Doppler-shift attenuation.  $^{11}\text{C}$  levels deduced  $\gamma$ -ray branching ratios,  $\tau_m$ .  $^{11}\text{B}$  level deduced  $\tau_m$ . Ge(Li) detector, enriched targets.

### I. INTRODUCTION

In terms of the shell model the lowest-order configurations of  $^{11}\text{B}$  and  $^{11}\text{C}$  are described by the term  $(1s)^4(1p)^7$ , which will only give rise to states of negative parity. Considerable effort has been made in these mirror nuclei to identify and describe their level structure.<sup>1</sup> In comparison with the situation in  $^{11}\text{B}$ , the lifetimes of these negative parity states in  $^{11}\text{C}$  are poorly known, and only upper limits of the order of 0.1–0.5 ps have been reported.<sup>1</sup> Improved transition strengths are clearly needed when testing the configurations proposed in different shell-model calculations.<sup>2,3</sup>

It appeared advantageous to use the method developed in our laboratory (e.g., Ref. 4) to determine the lifetimes of the negative parity states in  $^{11}\text{C}$ .

The experimental arrangement is described in Sec. II, and Sec. III presents the measurements and results. The transition rates are discussed in Sec. IV.

### II. EXPERIMENTAL

In the measurements, the 2.5 MV Van de Graaff accelerator at Helsinki University was employed. The energy resolution of the 50  $\mu\text{A}$  proton beam used was 1 keV. The 90° analyzing magnet was calibrated using the  $^{27}\text{Al}(p,\gamma)^{28}\text{Si}$  resonances at  $E_p = 773.70 \pm 0.03$ ,  $991.88 \pm 0.04$ , and  $1316.88 \pm 0.07$  keV.<sup>5</sup> The targets were prepared by implanting a 9  $\mu\text{g}/\text{cm}^2$  dose of 100 keV  $^{10}\text{B}^+$  ions into 0.4 mm

thick Ta backings in the isotope separator of the laboratory. The  $\gamma$ -ray radiation was detected with a Princeton 110  $\text{cm}^3$  Ge(Li) detector with an energy resolution of 1.9 keV at  $E_\gamma = 1.33$  MeV and 2.9 keV at  $E_\gamma = 2.61$  MeV and with an efficiency of 21.8%. The detector was mounted on a turntable centered on the beam spot on the target. Standard signal amplifying and analyzing equipment was used in conjunction with the detector. The stability of the spectrometer was checked with the  $^{40}\text{K}$  laboratory background peak, a  $^{208}\text{Tl}$   $\gamma$ -ray source, and with the accurately known  $\gamma$ -ray transition from the  $^{19}\text{F}(p,\alpha\gamma)^{16}\text{O}$  reaction.<sup>6</sup> The intensity measurements were performed at an angle of 55° relative to the beam direction and the DSA measurement at the angles of 0°, 30°, 45°, 60°, and 90°, while in addition angular distribution measurements were made at 120° and 135°. In order to reduce the solid angle corrections, the beam spot on the target was collimated down to 3 mm and a target-to-detector distance of 6 cm was used in all measurements.

### III. MEASUREMENTS AND RESULTS

#### A. Branching ratio and angular distribution data

The broad  $^{10}\text{B}(p,\gamma)^{11}\text{C}$  resonance ( $\Gamma_{\text{lab}} = 500 \pm 50$  keV<sup>1</sup>) at  $E_p = 1145 \pm 5$  keV corresponding to the  $E_x = 9732 \pm 5$  keV state in  $^{11}\text{C}$  is reported to be<sup>1</sup> the only resonance below the giant resonance region at  $E_p > 2.5$  MeV, and is used to populate the negative parity bound states in  $^{11}\text{C}$ . The  $\gamma$ -decay scheme of this resonance has previously been examined using a NaI(Tl) detector.<sup>7</sup> Because of the availability of

the large volume Ge(Li) detector, the  $\gamma$ -decay scheme was restudied in order to improve the experimental data on the feeding transitions to the bound levels in  $^{11}\text{C}$ . The sample  $\gamma$ -ray spectrum recorded at  $E_p = 1110$  keV with an accumulated charge of 1.5 C is shown in Fig. 1. A 1.1 cm thick lead absorber was interposed between the target and the detector in order to minimize the effects on the counting system of the high counting rate from the 431 keV  $\gamma$  rays yielded by the tail of the broad ( $\Gamma_{\text{lab}} \sim 250$  keV)  $^{10}\text{B}(p, \alpha_1 \gamma)^7\text{Be}$  resonance at  $E_p = 1.53$  MeV and of the 478 keV  $\gamma$  rays emitted in the 53 day  $\beta$  decay of  $^7\text{Be}$ .

Because of the total width of the  $E_x = 9.73$  MeV resonance state it is not possible to use a background spectrum, recorded below the resonance, in the identification of the relevant  $\gamma$ -ray transitions. Consequently,  $\gamma$ -ray identification was started by comparing the intensities of the tentative primary transitions with the secondary transitions according to the branching ratios given by Ajzenberg-Selove.<sup>1</sup> The efficiency of the detector

was determined in the experimental geometry with the  $\gamma$ -ray transitions in  $^{56}\text{Co}$ <sup>8</sup> and using relative  $\gamma$ -ray intensities in the  $^{27}\text{Al}(p, \gamma)^{28}\text{Si}$  reaction at  $E_p = 992$  keV.<sup>9</sup> The relative intensities as obtained for the primary transitions from the spectrum of Fig. 1 are summarized in Table I. In the cases of the  $\gamma$  transitions to the  $E_x = 4.32$ , 4.80, and 6.48 MeV states, at least the stronger of the secondary transitions were observed and the intensities corrected with the branching ratios<sup>1</sup> were in good agreement with those of the primary transitions. The relative intensity ( $0.4 \pm 0.2$ )% of the 2.00  $\rightarrow$  0 MeV transition seen in the spectrum can be explained by the ( $17 \pm 4$ )%<sup>1</sup> branch from the  $E_x = 4.80$  MeV state. The secondary transition 8.43  $\rightarrow$  0 MeV was observed with the intensity ( $80 \pm 20$ )% relative to the feeding transition  $r \rightarrow 8.43$  MeV. According to the analog nature of the  $E_x = 8.82(\frac{5}{2}^-)$  MeV state in  $^{11}\text{B}$ , an explanation of the unknown 20% decay could be  $\alpha$  decay.<sup>1</sup> For this, however, there is no experimental evidence, only the  $\gamma$  decay of the 8.43 MeV state being reported.<sup>1</sup> In spite of the

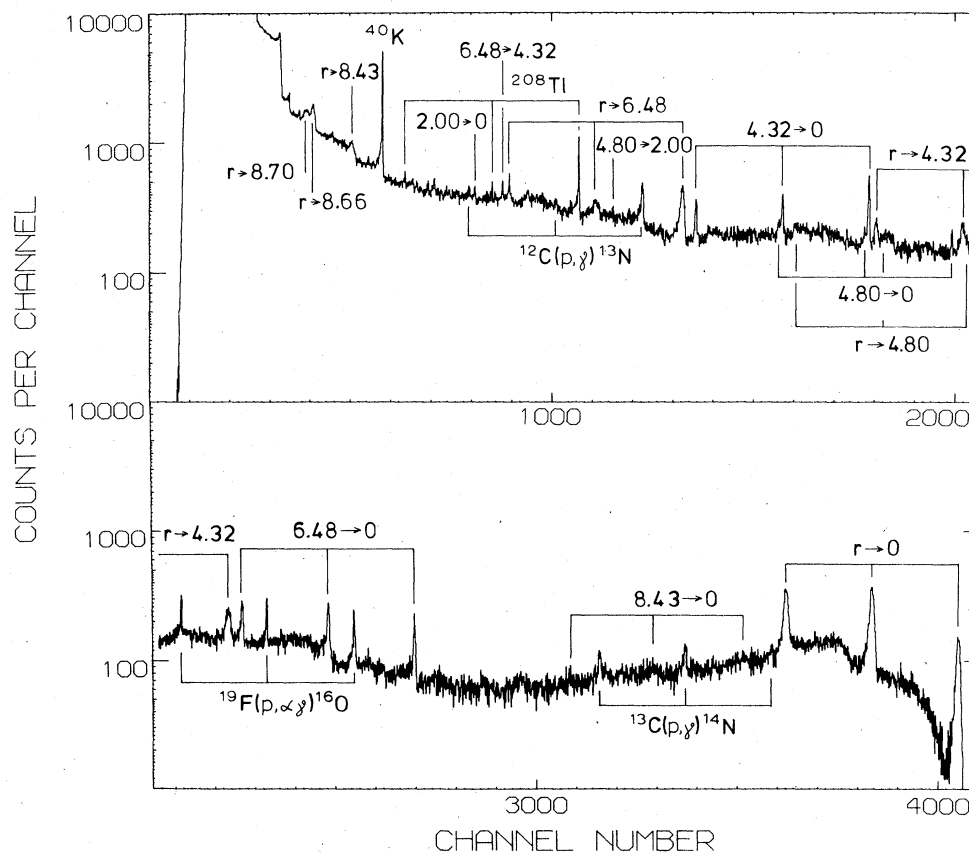


FIG. 1.  $\gamma$ -ray spectrum obtained in the  $^{10}\text{B}(p, \gamma)^{11}\text{C}$  reaction at  $E_p = 1110$  keV. The identification of the observed  $\gamma$ -ray transitions is shown, and  $r$  indicating the initial level energy at  $E_p = 1110$  keV corresponding to an excitation of 9701 keV in  $^{11}\text{C}$  (for the inclusion of the direct capture process; see text).

TABLE I.  $\gamma$  decay scheme of the  $^{10}\text{B}(p,\gamma)^{11}\text{C}$  reaction obtained at  $E_p=1110$  keV, and comparison with the previous branchings reported for the  $E_x=9.73$  MeV compound state.<sup>a</sup>

$E_f$ (MeV)	$J_f^\pi$	Relative intensity (%)	
		Present <sup>b</sup>	Ref. 7 <sup>c</sup>
0	$\frac{3}{2}^-$	$47.9 \pm 1.9^d$	$63 \pm 13$
2.00	$\frac{1}{2}^-$		(3)
4.32	$\frac{5}{2}^-$	$11.7 \pm 0.7$	$12 \pm 2$
4.80	$\frac{3}{2}^-$	$2.1 \pm 0.4$	(3)
6.48	$\frac{7}{2}^-$	$12.6 \pm 0.7^d$	19
8.43	$\frac{5}{2}^-$	$2.5 \pm 0.2^d$	
8.66	$\frac{7}{2}^+$	$13.7 \pm 0.8^e$	
8.70	$\frac{5}{2}^+$	$9.5 \pm 0.7^e$	

<sup>a</sup>The  $E_f$  and  $J_f^\pi$  values are taken from Ref. 1.

<sup>b</sup>Values are given as obtained at  $55^\circ$  relative to the beam (see text).

<sup>c</sup>Obtained at  $0^\circ$  and  $90^\circ$  relative to the beam and corrected for the measured angular distribution.

<sup>d</sup>Contributed by the E1 transition of the direct proton capture process (see text).

<sup>e</sup>E1 transition of the direct proton capture process (see text).

strong  $r \rightarrow 8.66$  and  $r \rightarrow 8.70$  MeV transitions as identified in Fig. 1, no secondary transitions were seen. The decay modes are unknown also in the literature, the  $\gamma$ -decay mode being assumed for the 8.66 MeV state. In order to confirm the identification of the  $r \rightarrow 8.43$ ,  $r \rightarrow 8.66$ , and  $r \rightarrow 8.70$  MeV transitions, seen for the first time in the present work, the  $\gamma$ -ray spectra were recorded at the energies  $E_p=1007$  and  $1200$  keV with an accumulated charge of  $1.5$  C. The peak positions and the same relative intensities as obtained at  $E_p=1110$  keV supported the identifications, which were manifested by the peak widths seen as the broadest peaks in the  $\gamma$ -ray spectra. After the deconvolution of the experimental resolution obtained from secondary transitions, the FWHM values yielded at  $E_p=1.11$  MeV to the target thickness the value of  $28 \pm 2$  keV. The  $\gamma$ -ray peak of the  $r \rightarrow 8.70$  MeV transition which is affected also by the width  $\Gamma = 15 \pm 1$  keV<sup>1</sup> of the 8.70 MeV state was seen to have a width  $32 \pm 2$  keV. In order to have a more rigorous identification a new target was made by implanting a  $5 \mu\text{g}/\text{cm}^2$  dose of  $20$  keV  $^{10}\text{B}^+$  ions into a  $0.4$  mm thick tantalum backing and a  $1.5$  C  $\gamma$ -ray spectrum was recorded at  $E_p=1110$  keV. Now the peak widths of the primary transitions narrowed down so that the target thickness of  $10 \pm 1$  keV was obtained, and the  $r \rightarrow 8.70$  MeV transition had the peak width  $18 \pm 2$

keV. Thus, it can be concluded that the intensities given in Table I belong to the transitions indicated and require revision of the previous  $\gamma$ -decay scheme of the  $E_x=9.73$  MeV state in  $^{11}\text{C}$ . The disappearance of secondary transitions from the  $E_x=8.66(\frac{7}{2}^+)$  and  $8.70(\frac{5}{2}^+)$  MeV states may be explained by the analog nature of these states with the  $E_x=9.19(\frac{7}{2}^+)$  and  $9.28(\frac{5}{2}^+)$  MeV states in  $^{11}\text{B}$ ,<sup>1</sup> which have been reported to decay mainly through  $\alpha$  particles.

Efforts to study the primary transitions in more details at proton energies above  $E_p=1200$  keV and below  $1007$  keV did not succeed. In order to learn more about the primary transitions given in Table I, angular distribution measurements were performed at  $E_p=1110$  keV at angles of  $0^\circ$ ,  $30^\circ$ ,  $45^\circ$ ,  $60^\circ$ ,  $90^\circ$ ,  $120^\circ$ , and  $135^\circ$ . The eccentricity of the measuring geometry was checked by the isotropic angular distribution of the  $7.90$  MeV  $\gamma$ -rays at the  $E_p=620$  keV,  $J^\pi=\frac{1}{2}^+$  resonance in the  $^{30}\text{Si}(p,\gamma)^{31}\text{P}$  reaction<sup>5</sup> and, (when the proton beam was removed from the target), by using the  $478$  keV  $\gamma$  rays produced from the  $53$  day  $\beta$  activity of  $^7\text{Be}$ . In order to know the absorption of the asymmetric target holder at the angles of  $120^\circ$  and  $135^\circ$ , the  $12.54$ ,  $6.02$ ,  $4.50$ ,  $2.84$ , and  $1.78$  MeV  $\gamma$  rays from the  $^{27}\text{Al}(p,\gamma)^{28}\text{Si}$  resonance at  $E_p=992$  keV were recorded several times at the angles of  $30^\circ$ ,  $120^\circ$ ,  $45^\circ$ , and  $135^\circ$ . In this way the eccentricity and absorption corrections were found to be less than  $3\%$  over the  $\gamma$ -ray energy region of the transitions given in Table I. In the angular distribution measurements the radiation yields were controlled by monitoring the intensity of the  $431$  keV  $\gamma$ -ray transition with a fixed  $66$  cm<sup>3</sup> Ge(Li) detector positioned at a distance of  $70$  cm from the target. The measured angular distributions shown in Fig. 2 were fitted to the expression  $W(\theta)=a_0[1+A_1P_1(\cos\theta)+A_2P_2(\cos\theta)]$ . In order to check the angular distributions of the  $r \rightarrow 8.66$  and  $r \rightarrow 8.70$  MeV transitions, which have low intensities at the angles  $0^\circ$ ,  $30^\circ$ ,  $45^\circ$ , and  $135^\circ$ , the narrow  $20$  keV  $^{10}\text{B}^+ \rightarrow \text{Ta}$  target was also employed in the angular distribution measurements. In this case the ratio of the peak height to the background was higher, and owing to the narrower  $\gamma$  peaks the uncertainties of the background effected less to the intensities. The fit yielded the angular distribution coefficients  $A_1$  and  $A_2$  which, corrected for the finite detector solid angle, are given as  $a_1$  and  $a_2$ , respectively, in Table II. The  $r \rightarrow 6.48$  MeV transition can be seen to have an unambiguous  $P_1(\cos\theta)$  term. In the cases of the  $r \rightarrow 0$  and  $r \rightarrow 8.43$  MeV transitions the  $P_1(\cos\theta)$  terms are also seen, their indisputability being not so clear. As the inclusion of the  $P_1(\cos\theta)$  term in the fitting reduced the present  $a_2$  values, no direct comparison can be made with the  $a_2$  values obtained

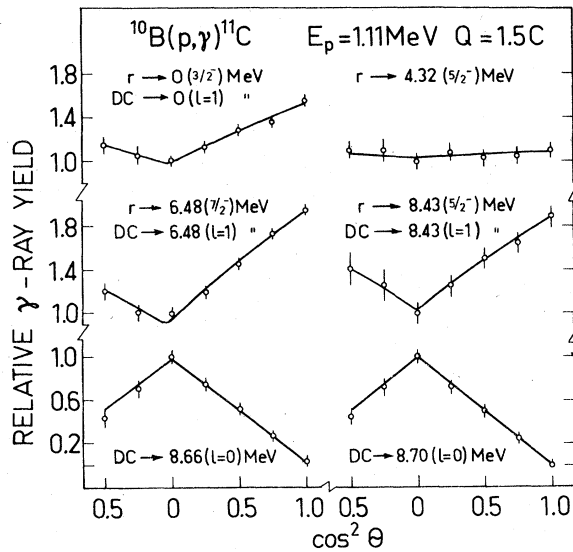


FIG. 2.  $\gamma$ -ray angular distributions of primary transitions obtained at  $E_p = 1110$  keV in the  $^{10}\text{B}(p, \gamma)^{11}\text{C}$  reaction. The possible  $E1$  direct capture contributions are indicated (see text).

in the previous  $^{10}\text{B}(p, \gamma)^{11}\text{C}$  study<sup>7</sup> where no forward-backward asymmetry was found in the  $r \rightarrow 0$ ,  $r \rightarrow 4.32$ , and  $r \rightarrow 6.48$  MeV transitions. The higher anisotropy seen in the present work for the  $r \rightarrow 0$  and  $r \rightarrow 6.48$  MeV transitions could be explained by the inclusion of the solid angle attenuation, see Table II.

The conflicting spin and parity assignments  $J^\pi = \frac{3}{2}^-, \frac{5}{2}^+$  of the compound state populated in the reactions  $^{10}\text{B}(p, \gamma)^{11}\text{C}$ ,  $^{10}\text{B}(p, p)^{10}\text{B}$ ,  $^{10}\text{B}(p, \alpha_0)^7\text{Be}$ , and  $^{10}\text{B}(p, \alpha_1 \gamma)^7\text{Be}$  at  $E_p \sim 1.15$  MeV have been illustrated by Overlay and Whaling<sup>11</sup> and  $J^\pi = \frac{3}{2}^-$  is considered to be a very improbable assignment. The proposed assignment  $\frac{5}{2}^+$  implies  $E1$  character for the  $r \rightarrow 0(\frac{3}{2}^-)$ ,  $r \rightarrow 6.48(\frac{7}{2}^-)$ , and  $r \rightarrow 8.43(\frac{5}{2}^-)$  MeV transitions which however, does not explain the  $a_1$  and the high  $a_2$  coefficients obtained in the present work. The significant single-particle spectroscopic factors (close to one) obtained in the  $^{10}\text{B}(d, n)^{11}\text{C}$  and  $^{10}\text{B}(\tau, d)^{11}\text{C}$  reactions for  $l=1$  proton strippings to the  $0(\frac{3}{2}^-)$ ,  $6.48(\frac{7}{2}^-)$ , and  $8.43(\frac{5}{2}^-)$  MeV states<sup>1</sup> suggest that the dominant  $E1$  transitions in the direct proton capture process from the  $l_p=2$  ( $J_r^\pi = \frac{5}{2}^+$ ) incoming partial wave could interfere with the  $l=1$  final state orbital angular momentum and produce the  $P_1(\cos\theta)$  term in the angular distributions (for details of the direct capture process, see Ref. 12). The  $r \rightarrow 4.32(\frac{5}{2}^-)$  MeV transition can be explained by the pure  $E1$  transition from the  $J_r^\pi = \frac{5}{2}^+$  compound state. The large single-particle spectroscopic factors of the

TABLE II. Summary of the angular distribution results for the  $^{10}\text{B}(p, \gamma)^{11}\text{C}$  reaction at  $E_p = 1.11$  MeV, and comparison with a previous  $(p, \gamma)$  study.<sup>7</sup>

Final state (MeV)	Present		Ref. 7
	$a_1^a$	$a_2^b$	$a_2^c$
0	$0.08 \pm 0.03$	$0.30 \pm 0.05$	$0.21 \pm 0.06$
4.32		$0.05 \pm 0.07$	$-0.17 \pm 0.08$
6.48	$0.16 \pm 0.05$	$0.49 \pm 0.05$	$0.40 \pm 0.04$
8.43	$0.04 \pm 0.08$	$0.45 \pm 0.09$	
8.66		$-1.06 \pm 0.07$	
8.70		$-1.12 \pm 0.06$	

<sup>a</sup>Solid angle corrections of the finite detector have been calculated in the present work to be about 3% and can be seen to be essentially smaller than the experimental uncertainties in the measurements.

<sup>b</sup>Solid angle corrections have been taken from Ref. 10. In order to check the solid angle corrections calculated for  $a_1$  coefficients, the corrections were calculated also for  $a_2$  coefficients and were found to be in agreement with those of Ref. 10.

<sup>c</sup>As obtained from the  $I(0^\circ)/I(90^\circ)$  ratio. No solid angle correction is included.

$8.66(\frac{7}{2}^+)$  and  $8.70(\frac{5}{2}^+)$  MeV states obtained in the  $l=0$  proton strippings<sup>1</sup> imply a significant direct  $E1$  capture into these states, from  $l_p=1$  incoming partial wave, with  $\gamma$ -ray angular distributions of the form  $W(\theta) \sim \sin^2\theta = 1 - P_2(\cos\theta)$ . The angular distributions obtained for both transitions are consistent with such an identification. As a consequence, a fraction of the observed  $\gamma$ -ray intensities as given in Table I for the  $r \rightarrow 0$ ,  $r \rightarrow 6.48$ , and  $r \rightarrow 8.43$  MeV transitions can be concluded to belong to the  $E1$  direct capture process and that the branching ratios given in Table I which are obtained in the  $^{10}\text{B}(p, \gamma)^{11}\text{C}$  reaction at  $E_p = 1.11$  MeV are obviously not the correct branches of the single  $E_p = 1145 \pm 5^1$  keV resonance, but are nevertheless relevant for the lifetime measurements. In order to untangle the resonant and nonresonant contributions to the  $\gamma$ -ray intensities observed a more detailed study should be done.

#### B. Lifetimes in $^{11}\text{C}$

In order to avoid the disturbing effects of the angular distributions the DSA measurements were performed at the angles of  $0^\circ$  and  $90^\circ$ . The measurements were repeated several times. The present  $F(\tau)$  values with the deduced mean lifetimes are given in Table III. The accumulated charge collected in the measurements was 1.5 C. The DSA measurement of the 4.32 MeV state is illustrated in Fig. 3. Photopeaks, single escape, and double escape peaks were used in the deduction of Doppler shifts when seen. The corrections for

TABLE III. Mean lifetimes observed for levels in  $^{11}\text{C}$  and comparison with previous values. The energy values are taken from Ref. 1.

$E_x$ (MeV)	$E_\gamma$ (MeV)	$F(\tau)$ (%)	Present <sup>a</sup>	$\tau_m$ (fs) Previous <sup>b</sup>	Adopted
2.00	2.00	$86 \pm 12^c$	$<34^c$	$<500$	$<34$
4.32	4.32	$93 \pm 4^c$	$<12^c$	$<140$	$<12$
4.80	4.80	$97 \pm 7$	$<11$	$<500$	$<11$
6.48	2.16	$96 \pm 2$	$4 \pm 2$	$<250$	$<8$
	6.48	$93 \pm 3$	$7 \pm 4$		
8.43	8.43	$92 \pm 11$	$<23$		$<23$

<sup>a</sup>The error limits of  $F(\tau)$ ,  $f_n$ , and  $f_e$  are included.

<sup>b</sup>As summarized in Ref. 1.

<sup>c</sup>The effect of feeding transitions is included.

solid angle attenuation were taken into account using the shifts of the primary  $\gamma$  rays. The  $r \rightarrow 0$  and  $r \rightarrow 4.32$  MeV transition yielded an average value of  $(99.8 \pm 1.2)\%$  for the full shift, where the average was taken over all cases studied. Although the primary lines were broad, their intensities were so high that the peak positions could be determined with an accuracy better than 3% compared to the full shift. The  $r \rightarrow 6.48$  MeV transition was rejected due to its high  $a_1$  term  $0.16 \pm 0.05$  (Table II).

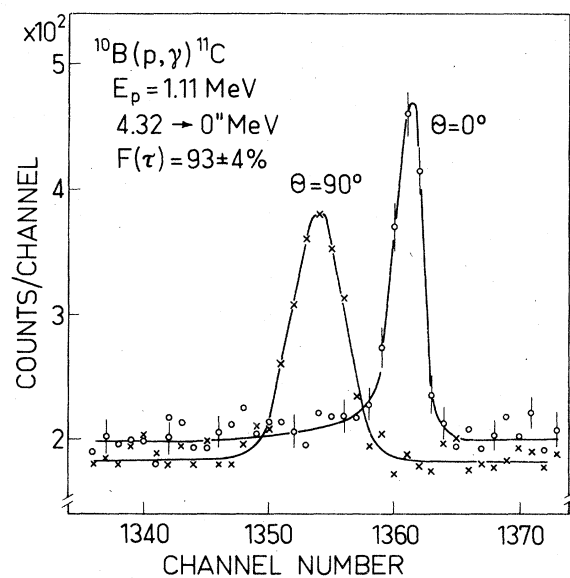


FIG. 3. Portions of  $\gamma$ -ray spectra recorded in the Doppler shift measurements of the  $4.32 \rightarrow 0$  MeV transition. The double escape peaks obtained at the angles of  $0^\circ$  and  $90^\circ$  relative to the beam direction are shown in the same figure. The photopeak and the single escape peak was overlapped by the  $4.80 \rightarrow 0$  MeV transition. The dispersion is  $2.38$  keV/ch.

The relevant data needed in the DSA analysis for description of the slowing down of the recoiling  $^{11}\text{C}$  nuclei were taken from our earlier study<sup>4</sup> where the correction factors of the nuclear ( $f_n$ ) and electronic ( $f_e$ ) stopping have been determined, in the frame of the LSS theory,<sup>13</sup> to be  $0.85 \pm 0.05$  and  $1.0^{+0.4}_{-0.3}$ , respectively, for the adjacent element  $^{14}\text{N}$ . These values were obtained by combining the range values of  $20$ – $100$  keV  $^{15}\text{N}^+$  ions in Ta, the attenuation factor  $F(\tau) = (26.4 \pm 0.9)\%$  and the line shape of the  $3891$  keV  $\gamma$ -ray peak from the  $6204$ – $2313$  keV transition in  $^{14}\text{N}$  recoiling in Ta measured using the  $E_p = 1150$  keV  $^{13}\text{C}(p, \gamma)^{14}\text{N}$  resonance. Because the range values of  $20$ ,  $40$ ,  $60$ ,  $80$ , and  $100$  keV  $^{13}\text{C}^+$  ions recoiling in Ta ( $56 \pm 3$ ,  $95 \pm 5$ ,  $121 \pm 7$ ,  $160 \pm 9$ , and  $187 \pm 10$   $\mu\text{g}/\text{cm}^2$ ,<sup>14</sup> respectively) are close to those ( $52 \pm 2$ ,  $81 \pm 4$ ,  $115 \pm 6$ ,  $139 \pm 7$ , and  $161 \pm 8$   $\mu\text{g}/\text{cm}^2$ ,<sup>4</sup> respectively) used in the deduction of the stopping parameters, the correction factors  $f_n = 0.85 \pm 0.10$  and  $f_e = 1.0 \pm 0.5$  with enlarged error limits can be expected to be valid also for the present case of  $^{11}\text{C}$ , where the dominant part of the uncertainties in the lifetime values arises from the  $F(\tau)$  values close to  $100\%$ . In the analysis Monte Carlo calculations with the above stopping power parameters were employed.

The present lifetime results are compared in Table III with the previous values obtained in  $^6\text{Li}(^6\text{Li}, n)^{11}\text{C}$  and  $^9\text{Be}(^3\text{He}, n)^{11}\text{C}$  measurements (see Ref. 1). In an unpublished work by Rosenthal *et al.*,<sup>15</sup> where the  $^{10}\text{B}(p, \gamma)^{11}\text{C}$  reaction was used, the  $4.32$  and  $6.48$  MeV states were reported to have lifetime values of  $<10$  fs, and the change of slowing down conditions yielded the limit  $<20$  fs.

### C. Lifetime in $^{11}\text{B}$

The only lifetime of the negative parity bound states in  $^{11}\text{B}$  which is not accurately known is the upper limit  $\tau_m < 10$  fs reported for the  $E_x = 6.74(\frac{7}{2}^-)$

MeV state.<sup>1</sup> Its analog state in  $^{11}\text{C}$ , the  $E_x = 6.48(\frac{7}{2}^-)$  MeV state was found in the present work to have a lifetime value of  $< 8$  fs. In the hope of improving the lifetime value of the 6.74 MeV state in  $^{11}\text{B}$  and of getting a comparison with the lifetime value of the 6.48 MeV state in  $^{11}\text{C}$ , the lifetime was remeasured in the present work through the  $^7\text{Li}(\alpha, \gamma)^{11}\text{B}$  resonance at  $E_\alpha = 0.96$  MeV. The DSA measurements performed at  $0^\circ$  and  $90^\circ$  are illustrated in Fig. 4. The target used was prepared in the isotope separator by implanting a  $3.5 \mu\text{g}/\text{cm}^2$  dose of 20 keV  $^7\text{Li}^+$  ions into Ta. The thickness of the target thus produced was  $4 \pm 1$  keV at  $E_\alpha = 0.96$  MeV obtained from  $\gamma$ -ray spectra. In calculating the experimental value  $F(\tau) = (94 \pm 2)\%$ , the solid angle attenuation was taken into account using the shift of the primary  $\gamma$  rays from the  $r \rightarrow 6.74$  MeV transition. Because of the lack of strong, narrow, isolated resonances in the  $^{10}\text{B}(p, \gamma)^{11}\text{C}$  or  $^{11}\text{B}(p, \gamma)^{12}\text{C}$  reaction,<sup>1</sup> no experimental correction factors for the nuclear and electronic stopping of  $^{11}\text{B}$  in tantalum can be obtained. In deducing the lifetime value  $\tau_m(E_x = 6.74 \text{ MeV}) = 15 \pm 6$  fs, a similar procedure as for the case of the  $^{11}\text{C}$  lifetimes was followed. The present lifetime is in agreement with the reported upper limits of 300,<sup>16</sup> 210,<sup>17</sup> and 40 fs.<sup>18</sup>

#### IV. DISCUSSION

The experimental transition strengths are given in Table IV along with the predictions of shell-

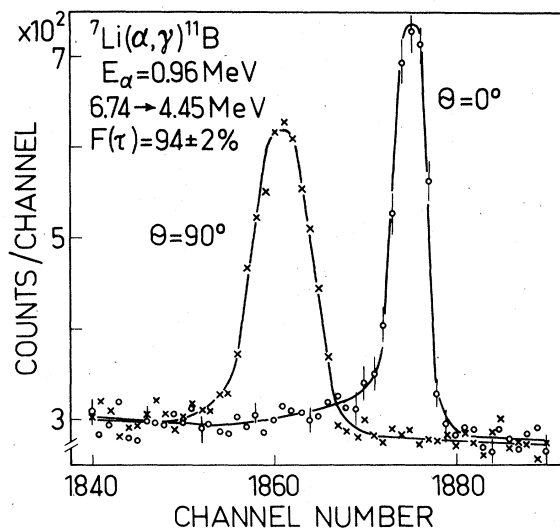


FIG. 4. Portions of  $\gamma$ -ray spectra recorded in the Doppler shift measurements of the 6.74  $\rightarrow$  4.45 MeV transition. The photopeaks obtained at the angles of  $0^\circ$  and  $90^\circ$  relative to the beam direction are shown in the same figure. The dispersion is 1.19 keV/ch.

model calculations. The theoretical values of  $M1$  transition strengths have been calculated mainly for  $^{11}\text{B}$  where experimental lifetime values have been known much better than in  $^{11}\text{C}$ . The theoretical  $M1$  strengths in  $^{11}\text{C}$ , as shown in Table IV, have been calculated from the wave functions obtained in a  $1p$  shell basis with the effective two-

TABLE IV. Experimental  $M1$  transition strengths<sup>a</sup> for negative parity states in  $^{11}\text{C}$  and their comparison with shell-model calculations.

$E_i$ (MeV)	$E_f$ (MeV)	$J_i^{\pi}$	$J_f^{\pi}$	$\tau_m^b$ (fs)	Branching (%)	$\delta$ ( $E2/M1$ )	$\Gamma_\gamma/\Gamma_w$ (W.u.)		
							Exp.	Ref. 2 <sup>c</sup>	Ref. 3
2.00	0	$\frac{1}{2}^-$	$\frac{3}{2}^-$	$< 34$	100		$> 0.012$	0.683	0.947
4.32	0	$\frac{5}{2}^-$	$\frac{3}{2}^-$	$< 12$	100	$+0.17 \pm 0.03^d$	$> 0.032$	0.201	0.218
4.80	0	$\frac{3}{2}^-$	$\frac{3}{2}^-$	$< 11$	$83 \pm 4$	e	$> 0.022$	0.557	0.560
	2.00		$\frac{1}{2}^-$		$17 \pm 4$	f	$> 0.022$	0.452	0.387
6.48	4.32	$\frac{7}{2}^-$	$\frac{5}{2}^-$	$< 8$	$11 \pm 3$	g	$> 0.02$	0.0102	0.0309
8.43	0	$\frac{5}{2}^-$	$\frac{3}{2}^-$	$< 23$	100	h	$> 0.0023$	0.276	0.436

<sup>a</sup> Unless stated otherwise, the experimental data are as summarized in Ref. 1.

<sup>b</sup> Present work.

<sup>c</sup> Determined from the (6-16)2BME interaction (Ref. 2).

<sup>d</sup> Excluding the phase, the value is in good agreement with the value of  $\delta = -0.19 \pm 0.03$  given in Ref. 1 to the analog transition.

<sup>e</sup>  $\delta = 0.03 \pm 0.05$  given in Ref. 1 to the analog transition is adopted.

<sup>f</sup>  $\delta = -0.05 \pm 0.2$  given in Ref. 1 to the analog transition is adopted.

<sup>g</sup>  $\delta = -0.45 \pm 0.18$  given in Ref. 1 to the analog transition is adopted.

<sup>h</sup>  $\delta = -0.11 \pm 0.04$  given in Ref. 1 to the analog transition is adopted.

body interaction computed through a least-squares fitting of free parameters<sup>2</sup> or through the Sussex relative harmonic-oscillator matrix elements.<sup>3</sup> The present lower limits of the  $M1$  strengths are, even if the feeding transitions with very short lifetimes are taken into account in the cases of the 2.00→0 and 4.32→0 MeV transitions, clearly below the theoretical ones, indicating by about a factor of 10 lower lifetime values to these states compared with the present upper limits. In order to illustrate how the lower limits and values for  $M1$  strengths would be effected by possible  $E2$  contributions, the experimental  $\delta(E2/M1)$  values as obtained for the analog transitions in  $^{11}\text{B}$ <sup>1</sup> are employed in the calculations of the strength values for the states 4.80, 6.48, and 8.43 MeV. The present upper lifetime limits of the 4.80 and 8.43 MeV states can be concluded to be by about a factor of 10 and 100, respectively, higher than the theoretical predictions.

In the case of the analog transitions  $6.48(\frac{7}{2}^-) \rightarrow 4.32(\frac{5}{2}^-)$  MeV in  $^{11}\text{C}$  and  $6.74(\frac{7}{2}^-) \rightarrow 4.45(\frac{5}{2}^-)$  MeV in  $^{11}\text{B}$ , the present experimental  $M1$  strengths  $>0.02$  and  $0.06 \pm 0.03$  W.u. are in mutual agreement and in agreement with the theoretical values of 0.0309 and 0.218 W.u.,<sup>3</sup> respectively, the theoretical values of Ref. 2, 0.0102 and 0.0066 W.u., respectively, being too small. The mixing ratio  $\delta(E2/M1) = -0.45 \pm 0.18$ <sup>1</sup> was employed in the calculations of both experimental  $M1$  strength values. No theoretical values are given for the strong  $E2$  transitions  $6.48(\frac{7}{2}^-) \rightarrow 0(\frac{3}{2}^-)$  MeV,  $(89 \pm 2)\%$ ,<sup>1</sup> and  $6.74(\frac{7}{2}^-) \rightarrow 0(\frac{3}{2}^-)$  MeV,  $(70 \pm 2)\%$ .<sup>1</sup> The present transition strengths  $|M(E2)|^2 > 4$  and  $= 1.9 \pm 1.0$  W.u., respectively, provide a further possibility to check the configuration of the initial  $\frac{7}{2}^-$  state at 6.48 MeV in  $^{11}\text{C}$  and at 6.74 MeV in  $^{11}\text{B}$  through the  $E2$  matrix elements which are more sensitive to configuration mixing than  $M1$  matrix elements.

<sup>1</sup>F. Ajzenberg-Selove, Nucl. Phys. A248, 1 (1975).

<sup>2</sup>S. Cohen and D. Kurath, Nucl. Phys. 73, 1 (1965).

<sup>3</sup>P. S. Hauge and S. Maripuu, Phys. Rev. C 8, 1609 (1973).

<sup>4</sup>M. Bister, A. Anttila, and J. Keinonen, Phys. Rev. C 16, 1303 (1977).

<sup>5</sup>P. M. Endt and C. van der Leun, Nucl. Phys. A214, 1 (1973).

<sup>6</sup>E. B. Shera, Phys. Rev. C 12, 1003 (1975).

<sup>7</sup>A. N. James, Nucl. Phys. 24, 675 (1961).

<sup>8</sup>M. Hautala, A. Anttila, and J. Keinonen, Nucl. Instrum. 150, 599 (1978).

<sup>9</sup>A. Anttila, J. Keinonen, M. Hautala, and I. Forsblom, Nucl. Instrum. 147, 501 (1977).

<sup>10</sup>D. C. Camp and A. L. van Lehn, Nucl. Instrum. 76, 192 (1969).

<sup>11</sup>J. C. Overley and W. Whaling, Phys. Rev. 128, 315 (1962).

<sup>12</sup>C. Rolfs, Nucl. Phys. A217, 29 (1973).

<sup>13</sup>J. Lindhard, M. Scharff, and E. Schiøtt, K. Dan. Vidensk. Selsk. Mat.-Fys. Medd. 33, No. 14 (1963).

<sup>14</sup>A. Anttila, M. Bister, A. Fontell, and K. B. Winterbon, Radiat. Eff. 33, 13 (1977).

<sup>15</sup>F. Rosenthal, J. Beyea, J. Lancman, and L. J. Lidofsky, Bull. Am. Phys. Soc. 14, 628 (1969).

<sup>16</sup>E. K. Warburton, J. W. Olness, K. W. Jones, C. Chasman, A. R. Ristinen, and D. H. Wilkinson, Phys. Rev. 148, 1072 (1966).

<sup>17</sup>M. J. Throop, Phys. Rev. 179, 1011 (1969).

<sup>18</sup>J. Beyea, H. Lancman, F. Rosenthal, and L. J. Lidofsky, Bull. Am. Phys. Soc. 14, 628 (1969).